

Bayesian item response models for citizen science ecological data.

Edgar Santos-Fernandez*

and

Kerrie Mengersen

School of Mathematical Sciences. Y Block, Floor 8, Gardens Point Campus.
Queensland University of Technology. GPO Box 2434. Brisbane
QLD 4001. Australia.

Australian Research Council Centre of Excellence for Mathematical and
Statistical Frontiers (ACEMS)

October 22, 2022

Abstract

So-called “citizen science” data elicited from crowds has become increasingly popular in many fields including ecology. However, the quality of this information is being fiercely debated by many within the scientific community. Therefore, modern citizen science implementations require measures of the users’ proficiency that account for the difficulty of the tasks. We introduce a new methodological framework of item response and linear logistic test models with application to citizen science data used in ecology research. A specific feature of this approach is that spatial autocorrelation is accommodated within the item difficulties. The models produce relevant ecological measures of species and site-related difficulties, discriminatory power and guessing behavior. These, along with estimates of the subject abilities allow better management of these programs. We found that the suggested methods outperform the traditional item response models in terms of RMSE, accuracy, and WAIC based on leave-one-out cross-validation on simulated and empirical data. The fit of item response models to big data via divide-and-conquer is also discussed. We illustrate the implementation using a case study of species identification in the Serengeti, Tanzania. The main R and Stan codes are provided in the supplementary materials section, which allows the reproducibility and extrapolation to other settings.

Keywords: ability estimation, big data, item response theory, latent variable regression, spatial model

*santosfe@qut.edu.au.

1 Introduction

Citizen science is becoming extremely valuable in modern science helping to overcome some of the limitations in conventional science settings (Raykar et al., 2010; Howe, 2008; Bonney et al., 2014). For example, large worldwide networks of participants are contributing to conservation efforts, generating large volumes of valuable information and achieving a better understanding and awareness (McKinley et al., 2017). The numerous examples found in the literature range from the worldwide estimation of the abundance of birds (Sullivan et al., 2009), to species of mammals in Africa (Swanson et al., 2015), the distribution of jaguars in the Peruvian Amazon (Mengersen et al., 2017) and hard coral cover estimation in the Great Barrier Reef (Peterson et al., 2019).

However, the quality of the data produced by volunteers is often questioned in the scientific community (Bonney et al., 2014; Kosmala et al., 2018). Contributors' commitment, abilities, training and effort along with the difficulty of the task affect their performance (Kelling et al., 2015; Dennis et al., 2017). In crowdsourcing projects, there is a growing interest in assessing how well users can perform estimation and classification tasks and specifically in measuring their latent abilities (e.g. Falk et al., 2019).

This can be approached using Item Response Theory (IRT) models, which are special cases of the family of generalized mixed models. There is an extensive literature on the use of IRT in multiple fields ranging from psychology, political and social sciences (Gadermann et al., 2012; Laurens et al., 2012; McGann, 2014), and education to statistics and computer sciences (Wauters et al., 2010; De Jong et al., 2010; van der Linden et al., 2010; Meyer and Zhu, 2013).

Multiple frequentist and Bayesian approaches to IRT have been employed, along with a wide range of computational methods. For example, for classification tasks, common models found in the literature are the logistic and normal models, while graded response models are employed for ordered categorical variables. Several implementations of Bayesian IRT models using different statistical languages have been also published. For instance, Curtis et al. (2010) used BUGS/JAGS, Grant et al. (2016); Luo and Jiao (2018) and Bürkner (2019) used Stan while Stone and Zhu (2015) employed SAS. Multiple examples can be found in Fox (2010) and in the Stan user manual (Carpenter et al., 2017).

Latent variable models that have been used in ecology to describe the occurrence of species as a function of latent predictors (Pollock et al., 2014; Warton et al., 2015) are distant cousins of the IRT models. However, not much attention has been paid to estimating the abilities and performance

measures for citizen science in ecological settings.

Measures of participants' abilities and their differentiation are relevant for several reasons. Statistical inference from crowdsourced data assigns greater weights to information from more competent users (Kosmala et al., 2016; Bird et al., 2014). In the absence of a gold standard, ability-derived weights can be used in consensus voting algorithms or for building reputation and leaderboard systems (Silvertown et al., 2015; Callaghan et al., 2019). Extremely low abilities are generally associated with careless, non-genuine respondents and bots which are generally excluded for being non-informative and representing a burden for inference and computation. Additionally, several crowd-sourcing platforms work on a compensation-based scheme founded on quality, for example in Amazon Mechanical Turk. Some projects also assign the task dynamically based on previous performance (Bachrach et al., 2012).

In this research, subjects are referred to as participants, citizens, annotators, users, while items refer to information sources (images, videos, audio files, etc.) (Zhang et al., 2013; Gura, 2013; Ratnieks et al., 2016). However, we concentrate on the particular case species identification on images.

Data collected in citizen science projects is challenging compared to what is found in the traditional item response literature. For example, the number of items for classifications can be large, reaching often hundreds of thousands and in some cases, it could be larger than the number of users. Additionally, participants score a different number of items. Some users engage heavily while others contribute lightly (Hsing et al., 2018). However, a user rarely scores all the items if the number is large. As a consequence, generally, a large proportion of data is missing. Overall, the skills of the respondents are generally heterogeneous, ranging from experts to beginners.

These complications are exacerbated when the focus of citizen science is on the classification of features or the identification of species in images. In this setup, camera, site, and species-specific factors can affect the underlying item difficulty level (Willi et al., 2019). Several image specific components maybe also critical e.g.: the camera resolution, brand, flash effect, etc. Other crucial factors are the visibility, time of the day (day or night), landscape and the vegetation. It has been also well documented that some species are far more difficult to identify than others. Look-alike or closely related species are more challenging, leading frequently to misclassifications (Chambert et al., 2018; Hsing et al., 2018).

In ecological research, items such as images are usually georeferenced (McKinley et al., 2017; Callaghan et al., 2019). An added complication in such a setting is that items that are geographically

close to each other tend to have more similar characteristics such as the probability of containing the target species, compared to those that are further away. Thus, latent image difficulties tend to exhibit spatial auto-correlation, which should be accounted for in the IRT models. Ignoring such autocorrelation can lead to biased parameter estimates and underestimating the associated standard errors and hence potentially erroneous inference.

The identification of areas with spatial correlation is also relevant for survey administration purposes. Distinguishing areas in which the items have relatively high difficulties is vital to provide recommendations on how to improve the quality of the images, generate more useful training and users' documentation, and to better manage the order in which tasks are presented for classification, etc. Images from camera traps difficult to identify might indicate technical issues. Additionally, identification of images with no visible species and covered by vegetation is relevant for data cleaning purposes.

A brief literature review

Since the introduction of the Rasch model (Rasch, 1960), several extensions and variations have been proposed for the IRT. The three parameter logistic model (3PL) (Birnbaum, 1968) and the graded response model by Samejima (1969) are among the most relevant contributions. Many examples and implementations can be found in widely known published textbooks e.g. Baker and Kim (2004); van der Linden and Hambleton (2013); Embretson and Reise (2013); De Ayala (2013). IRT modelling has been approached from the GLM perspective and a very didactic discussion can be found in Wilson et al. (2008). In a spatial context, Cançado et al. (2016) has suggested a model that borrows some principles of spatial statistics for the identification of spatial clusters. Another model accounting for changes in space and time is presented in Juhl (2019).

A new class of state-space model called dynamic item response is introduced by Wang et al. (2013) for longitudinal data. Under the principle that the abilities change over time, this dynamic approach produces a growth curve for the latent trait. Another dynamic IRT model was presented by Weng et al. (2018), where model parameters are updated as the data becomes available in a sequential manner.

Within the Bayesian philosophy, multiple model implementations have been suggested e.g. Patz and Junker (1999); Fox (2010); Albert (2015). Possibly the greatest limitation of Bayesian item response models is the identifiability issues arising from having a large number of parameters to be

estimated from the data. For a detailed discussion on identifiability see e.g. Fox (2010). Strategies like anchoring the sum or the mean of the difficulties to zero have been suggested to cope with this limitation.

In this research, we introduce extensions of the 3PL item response model (U)sing (S)patially dependent item difficulties (henceforth 3PLUS) and variations of the linear logistic test model (LLTM). These approaches are tailored to citizen science data elicited from georeferenced images. We discuss the advantages and limitations of the suggested methods. We take a Bayesian approach for modelling using prior information for the parameters of interest. This has multiple advantages which includes better parameter estimates for cases when the number of samples for some users is relatively small (Mislevy, 1986; Choy et al., 2009). We start with a simulation study to compare the proposed model to the state of the art. This is followed by a case study of citizen science image classification in the Serengeti, Africa.

2 Methods

In the case of citizen-elicited classification in an image, a common approach is to select points and ask the user whether each point contains the target class. Let the binary response variable Y represents whether the question was correctly answered by the i^{th} citizen ($i = 1, \dots, I$), in the j^{th} image ($j = 1, \dots, J$) for the k^{th} point ($k = 1, \dots, K$), $Y_{ijk} \sim \text{Bern}(p_{ijk})$.

In some cases the interest is on identifying species in the whole image and the above case is reduced to $k = 1$. The probability p_{ijk} of a correct answer can be modeled using the three-parameter logistic model (Lord, 1980; Baker and Kim, 2004).

$$p_{ijk} = \eta_j + (1 - \eta_j) \frac{1}{1 + \exp\{-\alpha_j (\theta_i - b_j)\}}. \quad (1)$$

Here θ_i is the latent ability of the i^{th} user, such that the higher the θ values are, the larger the probability of identifying correctly the class of the item. The parameter b_j represents the difficulty of the j^{th} image and $\alpha_j > 0$ represents the slope or discrimination parameter of image j indicating how quickly the function will go from 0 to 1. The parameter η_j is the *pseudoguessing* parameter of the j^{th} image that is the lower asymptote, which accounts for users' chance of answering correctly by guessing.

Several variations of this model can be found in the literature. For example, the two-parameter logistic (2PL) model is a reduction arising from setting $\eta = 0$, while the Rasch model is obtained

using $\eta = 0$ and $\alpha = 1$ (Cai et al., 2016). Another popular approach replaces the logistic link function by the probit link (Albert, 1992). The effect of these parameters on p is shown in Fig.1. Hence, the difficulty, slope and pseudoguessing parameter are considered locally homogenous within the image, so, the parameters b_j , α_j and η_j are common for each site k .

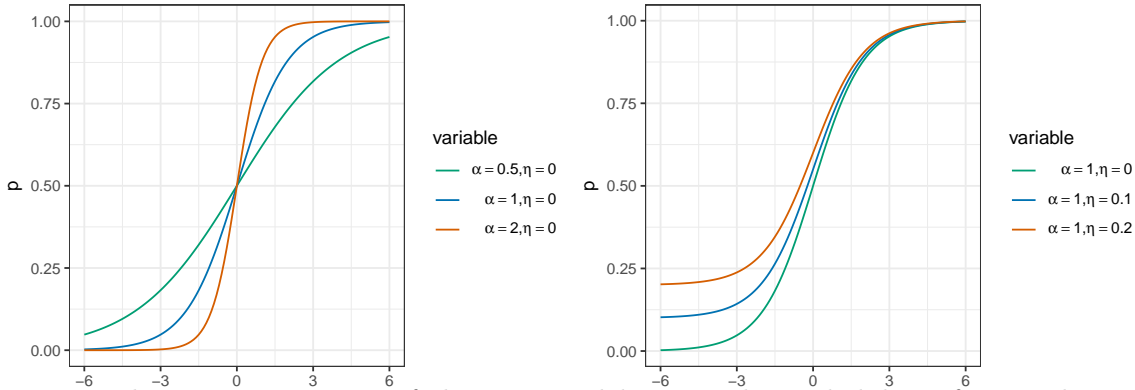


Figure 1: Item characteristic curves of the 3PL model giving the probability of correctly answering a standard item ($b = 0$) as a function of the latent user ability θ . In (a) we compare curves from three different values of the slope α with no guessing i.e. $\eta = 0$. In (b) we compare curves using three pseudoguessing values $\eta = 0, 0.1, 0.2$ and a fixed value of $\alpha = 1$.

In this paper, we suggest a spatial extension of the 3PL model in which we model the difficulties as a random spatial effect. We adopt a conditional autoregressive (CAR) prior (Besag et al., 1991), noting that the general approach can accommodate other representations of the spatial autocorrelation. Under the CAR prior, the distribution of b is normal with mean equal to the average of the neighbors and variance depending on the number of neighbors.

$$b_l | b_m, \tau_b \sim \mathcal{N} \left(\frac{1}{n_l} \sum_{l \sim m} b_m, \frac{1}{\tau_b n_l} \right) \quad (2)$$

where n_l is the number of neighbours for region l , $l \sim m$ means l and m are neighbours and $l \neq m$. The parameter τ_b is the precision of the spatial effect.

2.1 LLTM model extensions

We propose a further extension of the 3PLUS model called item explanatory, which is a special case of the linear logistic test model (LLTM) (Fischer, 1973; Wilson et al., 2008). In this approach, the item parameter (b_j) is a linear combination of factors governing the difficulty ($\sum_{m=1}^M \beta_m X_{jm}$), where M is the number of factors. This model does not give directly an indication of the difficulties associated with the images, but explains the effect of the item related factors. For instance, often we

are interested in the camera difficulty that accounts for the image quality and on the complications associated with the site (unique latitude and longitude) in which the camera is placed rather than on the individual image difficulties.

Similarly, the intrinsic difficulty associated with the species can be considered. This explains the misclassification error due to species that look like the target one and also mimic animal-specific behavior and features.

The probability that citizen i correctly identifies species l in the j^{th} site is given by:

$$p_{ijl} = \eta + (1 - \eta) \frac{1}{1 + \exp \{-\alpha \cdot (\theta_i - \beta_j I_j - \beta_l I_l)\}} \quad (3)$$

where I_j and I_l are indicator variables of the site and species respectively. The parameters β_j and β_l are difficulties associated with the site and species respectively.

The pseudoguessing η can be associated with the species or with the sites. The first case is more reasonable since it explains what species are more likely to be correctly classified due to guessing. High values of species-related pseudoguessing values indicate species that are easily classified for those users with less proficiency. Similarly, species or site-specific discrimination parameters can be estimated in the model (α_l or α_j), showing which items are more suitable for differentiating the users.

To avoid confusion, we will retain the notation previously used to refer to the models but we add a prime symbol (') to denote *test model* extensions. That is, the test model (3PLUS') of Eq.3 is an extension of the model introduced in Eq.1 with b_j replaced by $\beta_j I_j + \beta_l I_l$.

3 Simulation study

We first present a simulation study to compare the performance of the 3PL and 3PLUS models. Consider $j = 225$ unique geographical locations in a 15×15 grid, which is generally large enough for the illustration and has been employed in several practical designs e.g. (Swanson et al., 2015). For the image difficulties we generated the spatial autocorrelation using a multivariate normal distribution, $b_j \sim \text{MVN}, (\mu_b = 0, \Sigma_b)$, with a spatial covariance matrix Σ_b obtained using the simple exponential form e.g.: $\Sigma_b = \exp(-d/r)$, where d is the Euclidean distance between locations and r is a scaling parameter.

Fig.4 (a) shows the spatial association between the difficulties and regions characterized by clusters of images that are *easy* (light blue) and *hard* (dark blue) to classify. Consider five groups of

users with fixed abilities: $\theta_i = \{-1, -0.5, 0, 0.5, 1\}$. We set several values for the discrimination (α) ranging from small to large slopes, $\alpha_i = \{0.25, 0.50, \dots, 1.50, 1.75\}$. A pseudoguessing parameter $\eta \sim \text{Beta}(5, 25)$ is used considering that users have on average 1 in 6 chances of guessing the true target class. Generally, a weakly informative prior is used for this parameter.

A random user, slope and pseudoguessing value is assigned with replacement to each image id. Each citizen scores multiple images and each image is classified several times. Every image contains 15 elicitation points. Using p from Eq.1 we simulated binary realizations using the Bernoulli distribution.

3.1 Fitting the Bayesian models

We want to learn about the latent parameters θ , b , α and η using the observed variable (Y_{ijk}). We employ Markov chain Monte Carlo simulations, in particular Hamiltonian Monte Carlo (HMC), in the software package Stan (Carpenter et al., 2017) which is based on the no-U-turn sampler (NUTS) (Hoffman and Gelman, 2014). We used 3 chains each of 50,000 samples after we discarded a burn-in of 20,000 samples. We used the prior distributions shown in Fig 2. The CAR prior was implemented according to Morris et al. (2019).

$\theta_i \sim \mathcal{N}(0, \sigma_\theta)$	# hierarchical informative prior on the abilities
$\sigma_\theta \sim \text{uniform}(0, 10)$	# flat prior for the user's abilities sd
$b_{3PL} \sim \mathcal{N}(\mu_b, \sigma_b)$	# informative prior on the difficulties in 3PL model
$\mu_b \sim \mathcal{N}(0, 5)$	# normal prior for the mean of the item difficulty
$\sigma_b \sim \text{Cauchy}(0, 5) T(0,)$	# flat prior for the sd of the item difficulty
$b_{3PLUS} \sim \text{CAR}(\tau, W, D)$	# CAR prior for the spatial model
$\tau_b \sim \text{Gamma}(1, 1)$	# precision of the spatial effect
$\alpha \sim \mathcal{N}(1, \sigma_\alpha)$	# normal prior with mean 1 on the slope
$\sigma_\alpha \sim \text{Cauchy}(0, 5) T(0,)$	# half Cauchy prior for the slope sd, where $T(0,)$ means lower truncation at 0
$\eta \sim \text{beta}(1, 5)$	# weakly informative prior on the pseudoguessing
τ	# precision parameter in the CAR prior
$D_{m \times m}$	# diagonal matrix
$W_{m \times m}$	# adjacency matrix

Figure 2: Prior distributions used in the models.

The parameter b_{3PL} is the difficulty in the traditional model (3PL), while b_{3PLUS} represents the difficulty in the spatial approach. We anchored the ability of the “reference” user by setting it equal

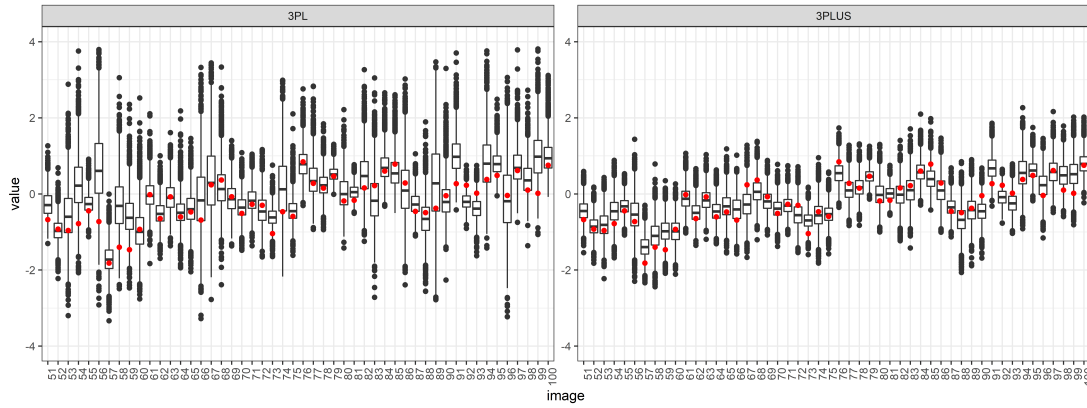
to zero. This was done by fitting the model in the *mirt* package (Chalmers, 2012) and finding the user with the score closest to zero.

The comparison of the models was based on the following criteria: (1) confusion matrix and the accuracy when estimating the parameters (difficulties, abilities, slopes, pseudoguessing), (2) Root Mean Square Error (RMSE), (3) WatanabeAkaike information criterion (WAIC) (Watanabe, 2010).

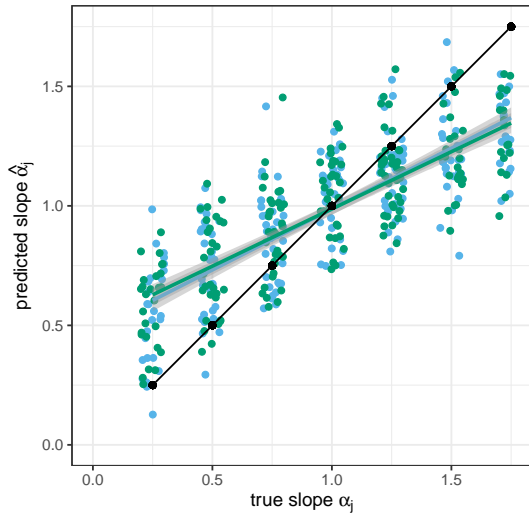
3.2 Simulation results

Both models produced similar user abilities estimates (See Fig S.12a and S.12b in the Supplementary Material). The RMSE for the 3PLUS model was slightly smaller (0.2036 vs 0.2092). The 3PLUS model produces substantially better difficulty estimates (Fig 3a and 4) with a better accuracy and precision. The yellow labels in Fig 4 (b) and (c) are the locations where the true difficulties estimates were not correctly identified. The 3PLUS model achieved an 80% prediction accuracy of the difficulty classes compared to 62.22% under the 3PL model. This model also halved the RMSE: $RMSE_{3PLUS} = 0.2596$ vs. $RMSE_{3PL} = 0.4808$. The correlations between the estimated difficulties and the true values were $r_{3PLUS}^2 = 0.9685$ vs $r_{3PL}^2 = 0.8776$. Both models produced similar estimates of the slope (α), but the pseudoguessing parameter (η) was better estimated in the 3PLUS model in terms of RMSE. See Fig 3b and 3c. The 3PLUS model also produces a slightly smaller WAIC (44,586.7 vs 44,637.0) and LOO (leave-one-out cross-validation) values (44,588.1 vs 44,638.7).

(a) Boxplot of the difficulties

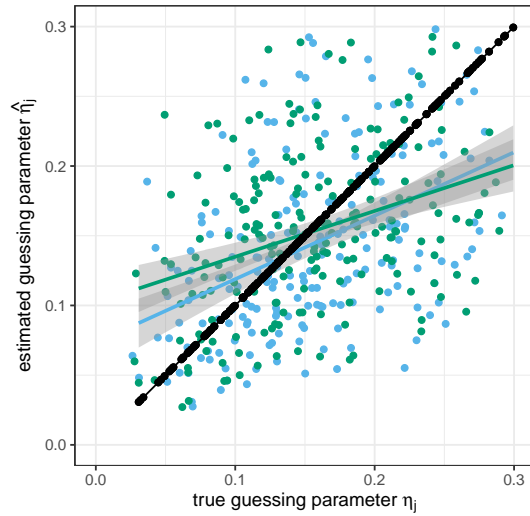


(b) Slope



Slope (alpha) 3PL model 3PLUS model

(c) Guessing



Guessing (eta) 3PL model 3PLUS model

Figure 3: (a) Boxplot of the estimated difficulties for locations 51-100. The true parameter value (red dots) in the traditional 3PL (left) and the 3PLUS model (right). Estimated slope (b) and guessing (c) parameters in the traditional 3PL (green) and the 3PLUS model (blue). The y-axis gives the estimates while the x-axis represents the true value. The ideal case of perfect estimation is represented in black color.

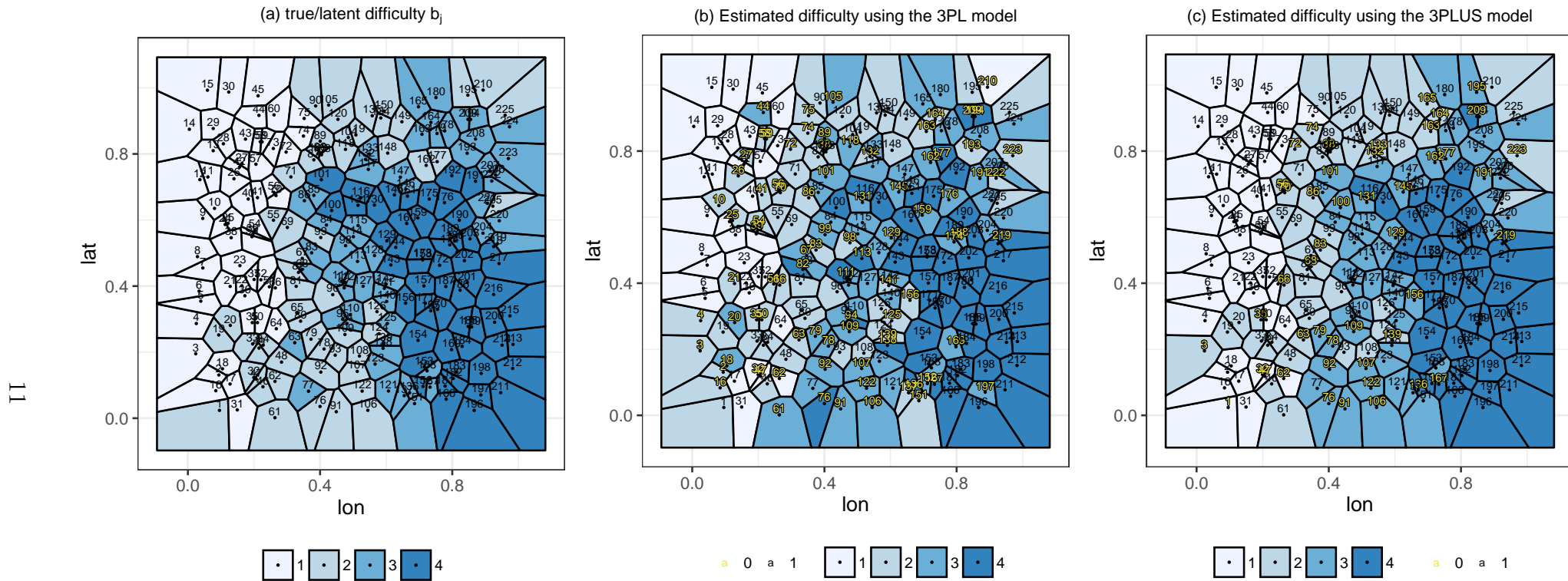


Figure 4: (a) Voronoi diagram of the latent spatially correlated item difficulties b_j . The color represents the difficulty category given by the quantiles $\{-2.178, -0.514\}$, $(-0.514, 0.232]$, $(0.232, 0.814]$, $(0.814, 1.982\}$ so that each category is composed of approximately 56 locations. The easiest and hardest groups are 1 and 4 respectively. (b) and (c) are the estimated item difficulties in the traditional 3PL and in the 3PLUS model. The yellow labels represent incorrect category estimation.

3.3 Effect of having more classifications

One of the main strengths of citizen science programs is the rapid acquisition of a large volume of classifications (Bonney et al., 2009). However, several issues relevant to these programs are not often quantified. For instance, how does the number of participants affect the precision of the estimates? How many sampled locations are needed? What is a suitable number of classifications per image? We designed an experiment to assess the effects of these three factors on the model fit and considered the following values:

1. grid size: This represents the number of unique geo-tagged locations for the items, e.g. image GPS coordinates: 10×10 , 15×15 and 25×25 .
2. number of participants: 9, 21 and 60. This was chosen to be very small, small and medium based on the impact or the precision of the estimates.
3. the number of elicitation points per image: This frequently arises in approaches used in ecology and is also known as the random point count methodology (e.g. Kohler and Gill, 2006) : 5, 15 and 25.

For this combination of parameters, we generated 27 datasets and fit both the 3PL and the 3PLUS models. Fig 5 depicts a comparison between the two models based on (a) RMSE of the difficulties and (b) the accuracy of retrieving the true category. The three grid sizes are represented with different line types. The panels show the number of users.

The proposed model produces a substantially smaller RMSE and better accuracy for most of the factor combinations. The greater the number of elicitations and users the smaller the RMSE and the larger the accuracy is in both models.

We fitted Bayesian regression models for the parameters (difficulties, abilities, slopes, and pseudoguessing) to the (log) RMSE as a function of the factors plus the model type using as a baseline factor the benchmark (3PL). The posterior density and trace-plots showed well-mixed chains and convergence.

In the model for the log RMSE of the difficulties, there are more differences between the models than when accounting for the factors. The numbers of elicitations, citizens and the grid size were found to affect the RMSE.

We found similar outcomes for the models using as a response variable the RMSE in the abilities, slopes, and pseudoguessing. A negative value in the model dummy variable means that a reduced RMSE is obtained when using the 3PLUS model. Larger numbers of elicitations and citizens also decrease the RMSE.

Fig 5 compares the RMSE of the difficulties, abilities, slopes and pseudoguessing parameters and the accuracy retrieving the difficulties in both models. The 3PLUS model produces smaller RMSE and the difference tends to be proportional to the number of users and the grid size.

New algorithms are often computationally intensive and involve larger processing times. We performed the simulations on a High-Performance Computing (HPC) system with CPUs architecture Intel AVX and AVX-2. No substantial differences in computing times were found between models.

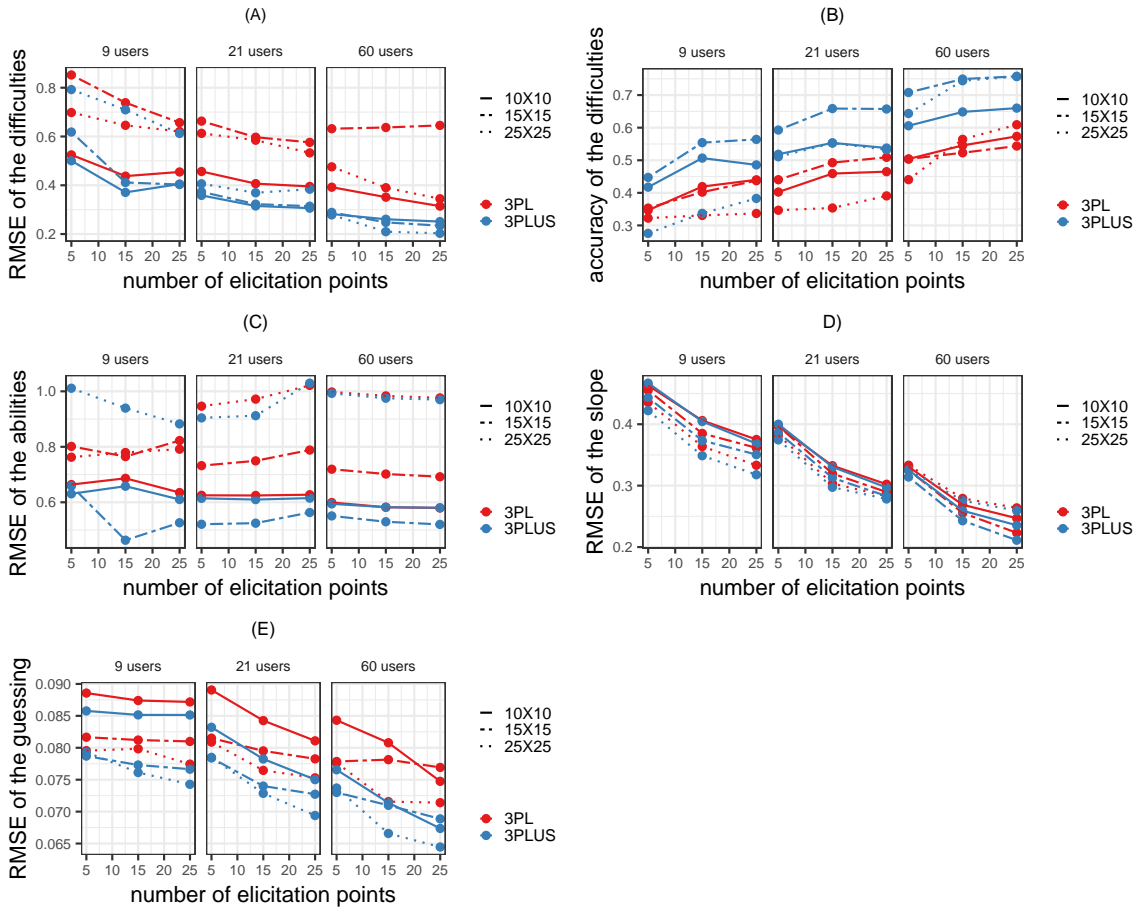


Figure 5: Root mean square error (RMSE) of the difficulties (A), abilities (C), slopes (D) and pseudoguessing (E) and difficulties accuracy (B) for each model (3PL vs 3PLUS). The x-axis represents the number of elicitation points/image and the panels give the number of users on each group. The grid size is plotted with different line types.

Table 1: Posterior summary statistics of the regression model for the $\log(\text{RMSE}_{\text{diff}})$.

Parameter	Rhat	n_eff	mean	sd	se_mean	2.5%	50%	97.5%
$b_{\text{Intercept}}$	1.0012	3614	-0.2905	0.0786	0.0013	-0.4452	-0.2912	-0.1376
$b_{\text{model3PLUS}}$	1.0006	3035	-0.4437	0.0429	0.0008	-0.5275	-0.4439	-0.3602
b_{neli}	1.0003	5022	-0.0088	0.0027	0.0000	-0.0141	-0.0088	-0.0035
$b_{\text{min}_{\text{clas}}}$	0.9999	3226	-0.0021	0.0077	0.0001	-0.0170	-0.0022	0.0128
$b_{\text{n}_{\text{cst}}}$	0.9994	5967	-0.0086	0.0010	0.0000	-0.0106	-0.0086	-0.0066
b_n	1.0015	4111	0.0003	0.0001	0.0000	0.0001	0.0003	0.0005
σ	1.0010	2558	0.2774	0.0156	0.0003	0.2487	0.2766	0.3099
log-posterior	1.0016	1590	-28.1311	1.8649	0.0468	-32.6632	-27.8176	-25.5008

4 *Hakuna my data: A case study of species identification in the Serengeti*

4.1 The Serengeti data

Swanson et al. (2015) describe a citizen science project that identified species from the Serengeti, Tanzania. This project is hosted on Zooniverse (<https://www.zooniverse.org/projects/zooniverse/snapshot-serengeti>). They captured more than a million images, with a total of 10.8 million classifications produced by 28,000 users. Images were obtained by camera traps in 225 spatial locations.

This dataset contains image details of the classifications per user and includes the spatial component given by the location of the cameras. The authors published several datasets including the original raw classification data, the consensus voting results and a gold standard dataset. The gold standard dataset included classifications by experts of 4,140 images.

A total of 50 species categories were identified including wildebeest, zebra, buffalo, hartebeest, lion (female and male), etc. The categories *impossible* to identify and *human* were also included. The authors noted that subjects tend to use more the *nothing here* classification rather than guessing when they were not sure of the species. Two-dimensional kernel density plots of the three most abundant species (prey) plus female lion (predators) is shown in Fig 6.

Images were captured at different times of the day, including night time. A sequence of three images was shown for daylight images, which helps in identifying the true species. Several other factors affecting the difficulty of the images are included: animal moving or feeding, the presence of babies, the relative position regarding the vegetation and camera placement, etc.

We selected the registered users with more than five classifications so that we can obtain suitable estimates of the abilities. For inclusion, images had to have a known location or site id. This produced a dataset composed of almost 5 million observations, from 21,347 citizens from 225 locations.

4.2 Analysis using the gold standard data and model comparison

Assessing the fit of several model variations and comparisons becomes difficult with large datasets. We first find the best performing model using the gold standard dataset and then fit it using the whole data. For simplicity, images with more than one species were excluded resulting in 88,517

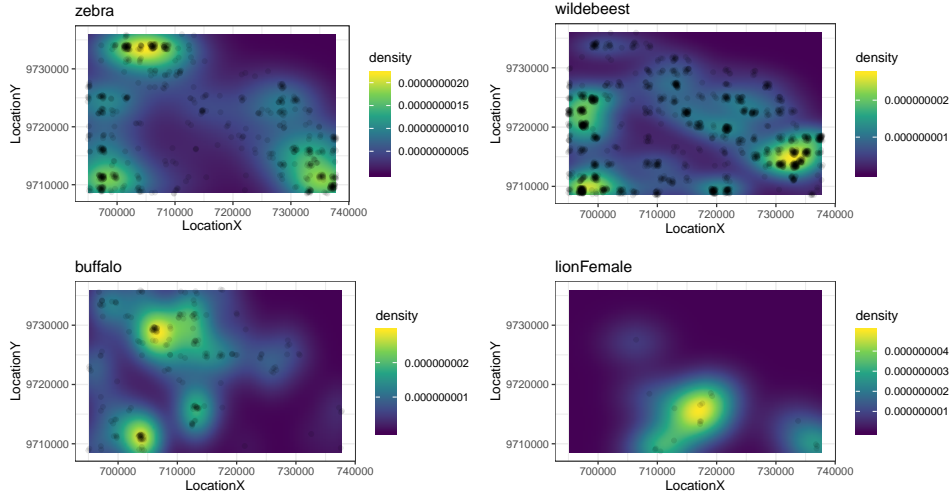


Figure 6: 2D kernel density plot of the three most abundant species (prey) in the gold standard dataset plus female lion (predators).

observations.

We considered 10 model variations of Eq.3, shown in Table 2. The 10 competing models were fit in Stan using four chains, 4000 iterations and a burn-in of 2000 reaching convergence. The estimates for the effective number of parameters \hat{p}_{waic} were found to be unreliable, exceeding 0.4 (Vehtari et al., 2017), for which using leave-one-out cross-validation (LOO) is recommended. The LOO measure also seems appropriate since we are interested in the applicability to other users/items. See Table 2.

According to the LOO information criterion values, the 3PLUS-2' model seems to be superior. In this model, the pseudoguessing parameter is species-related, while the slope is indexed to the site that accounts for the camera and location-specific factors.

Table 2: Model variations from the model in Eq.3 ($p_{ijl} = \eta_i + (1 - \eta_i) \frac{1}{1 + \exp\{-\alpha_i(\theta_i - \beta_j I_j - \beta_l I_l)\}}$) where the citizen is indexed by i , the site location by j and the species by l . The symbol ' indicates test model extension.

Model	Name	Parameters	WAIC	LOO
3PL	traditional 3PL model	$\eta_l, \alpha_l, \theta_i, \beta_l, \beta_j = 0$	94,396.2	94,443.9
3PLUS	spatial 3PL model	$\eta_j, \alpha_j, \theta_i, \beta_j \sim \text{CAR}(W, D, \tau)$ and $\beta_l = 0$	86,153.3	86,205.8
1PL'	traditional 1PL test model	$\eta = 0, \alpha = 1, \theta_i, \beta_l$ and β_j	86,167.6	86,197.2
2PL'	traditional 2PL test model	$\eta = 0, \alpha_j, \theta_i, \beta_l$ and β_j	85,401.2	85,453.6
3PL'	traditional 3PL test model	$\eta_j, \alpha_j, \theta_i, \beta_l$ and β_j	85,439.2	85,495.7
1PLUS'	spatial 1PL test model	$\eta = 0, \alpha = 1, \theta_i, \beta_l$ and $\beta_j \sim \text{CAR}(W, D, \tau)$	86,186.0	86,215.8
2PLUS'	spatial 2PL test model	$\eta = 0, \alpha_j, \theta_i, \beta_l$ and $\beta_j \sim \text{CAR}(W, D, \tau)$	85,411.2	85,463.3
3PLUS'	spatial 3PL test model	$\eta_j, \alpha_j, \theta_i, \beta_l$ and $\beta_j \sim \text{CAR}(W, D, \tau)$	85,419.6	85,474.8
3PLUS-2'	spatial 3PL test model	$\eta_l, \alpha_j, \theta_i, \beta_l$ and $\beta_j \sim \text{CAR}(W, D, \tau)$	85,199.3	85,257.9
3PLUS-3'	spatial 3PL test model	$\eta_l, \alpha_l, \theta_i, \beta_l$ and $\beta_j \sim \text{CAR}(W, D, \tau)$	85,711.2	85,766.9

4.3 Item response modeling for big data

Fitting item response models to big datasets can be challenging and prohibitive within the Bayesian paradigm. Operations involving a large number of parameters often exceed the memory, processing and disk capacities, which is exacerbated if simulation-based computation/estimation such as MCMC is used. This is even more problematic when accounting for spatial autocorrelation (Katzfuss and Cressie, 2012; Datta et al., 2016; Finley et al., 2017).

In this section, we focus on modelling datasets too large to be fit directly in one machine or even on a modern HPC node. We use the dataset previously described, which is composed of almost 5 million classifications. The true answer (species) was obtained in the non-gold standard images using the voting consensus.

We took a divide-and-conquer or a divide-and-recombine approach (Scott et al., 2016; Neiswanger et al., 2013; Wang et al., 2016) splitting the big dataset into multiple shards or subsets. Models were fit to the independent subsets on independent machines with no communication, and subposterior estimates were then combined into global estimates using consensus Monte Carlo (Scott et al., 2016). Specifically, we used weighted averages of the posterior MCMC chains, with weights inversely proportional to the variance of the posterior samples. At each iteration, the consensus estimate of a parameter is given by $\theta_g = \left(\sum_s^S W_s\right)^{-1} \sum_s^S W_s \theta_{sg}$, where s is the subset or machine, g is the iteration number, θ_{sg} is the estimate at the iteration g from the machine s and $W_s = \text{Var}(\theta|y_s)^{-1}$.

The consensus Monte Carlo is known to produce an asymptotic approximation to the posterior based on the whole dataset (Scott et al., 2016). However, multiple other options could have been explored to obtain the combined subposterior distributions (e.g. Neiswanger et al., 2013).

The number of observations of each location and species is large. However, the classifications per user varied from a few to several hundred. Thus, we employed stratified sampling with users as grouping criteria thereby splitting the dataset into 10 equal parts. This yielded 10 shards with approximately half a million observations per shard. Some users will not be represented on all the subsets, while most of the species and sites were estimated on every shard.

Shards were fitted in parallel with no communication on a high performance computing (HPC) system using 10 CPUs, three processors and a request of 280 Gb of memory. Estimates of the latent parameters were obtained using the best performing model (3PLUS-2') found in the previous section. We used three chains, a warm-up period of 3000 samples and 8000 iterations. It took approximately 42 hours to fit each model and to compute the WAIC.

For combining the subposteriors into the whole dataset posterior, we modified the function *consensusMCindep()* from the R package *parallelMCMCcombine* (Miroshnikov and Conlon, 2014).

This approach is suitable for normally distributed parameters (difficulties, abilities, slopes) and has been found to work satisfactorily also for non-normal variables (Scott et al., 2016) such as the pseudoguessing which is modelled using beta distributions. Summary statistics of some of the parameters of interest are shown in Table S.3.

On each machine, we obtained subposterior estimates for each of the parameters. For instance, in Fig 7 we show the estimates for nine users with good, moderate and poor classification skills (three on each group). In some cases, there could be a moderate variability on the estimates obtained from different shards e.g. user = 2. This is because by random, users will have a better performance in some subsets than in the others. See Fig S.13 for scatter plots comparing the posterior ability estimates in the 10 shards (abil1, abil2, etc.) and in the recombined consensus posterior (abil).

Fig 8 shows the user proficiency levels as a function of the proportion of correct classifications.

Similarly, we obtained posterior distributions for the difficulties in identifying the species (Fig 9a). Species with mean positive values are more difficult to identify e.g. hyena striped. Other

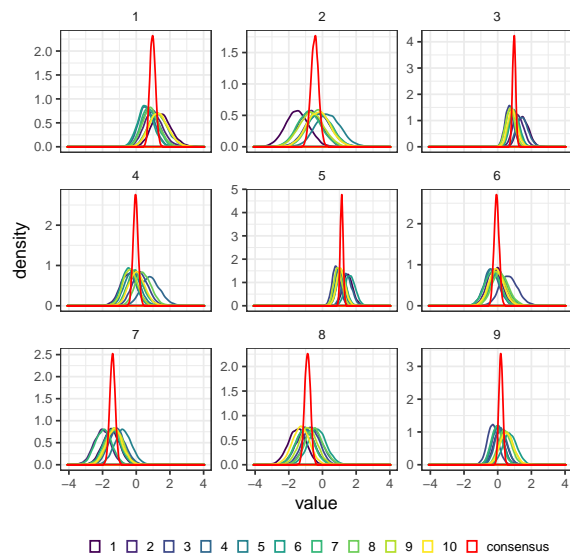


Figure 7: Posterior estimates of the abilities for nine users in 10 machines and the posterior obtained using the consensus approach (in red).

categories with negative estimates such as giraffe and zebra had a high probability of correct classification. Fig 9b shows the posterior estimates of the species difficulties as a function of the proportion of correct classification. On average citizens misclassified images containing humans with probability 0.10 and this could be considered as an indicator of careless respondents.

We also obtained the minimum probability of a correct answer for species due to guessing, for users with extremely low abilities (Fig.10a and 10b). Interestingly, large pseudoguessing estimates are obtained for lions, the only species for which the gender was required (female and male). These species had a higher probability of being correctly identified by less experienced users.

Fig S.15 displays scatter plots of the correlation between shards, showing a high correlation between the combined estimates (guess_all) and the ones obtained from the shards (guess1, guess2, etc.).

Site-related difficulties were also produced. Images from some sites were harder to classify; see for instance C05 in Fig.11a. A comparison between the 225 sites subposterior estimates among the 10 shards is presented in Fig.S.16. These results indicate a high degree of agreement between site difficulties obtained from the different subsets and compared to the consensus values.

In Fig 11b we show the posterior estimates of the site difficulties as a function of the proportion of correct classification and the Voronoi diagram of the site difficulties. Sites with a larger difficulty estimate could indicate camera-related problems or installation issues.

5 Discussion and conclusion

Networks with millions of contributors worldwide scattered in space and time engage in citizen science activities. This force is helping to reach the United Nations Sustainable Development Goals (Hsu et al., 2014; Fritz et al., 2019). In the ecological context, citizens' contribution is two-fold: providing images, videos and audio files from animals, plants, etc.; but also producing classifications for estimating the distribution of species and for training machine learning algorithms. Yet, the

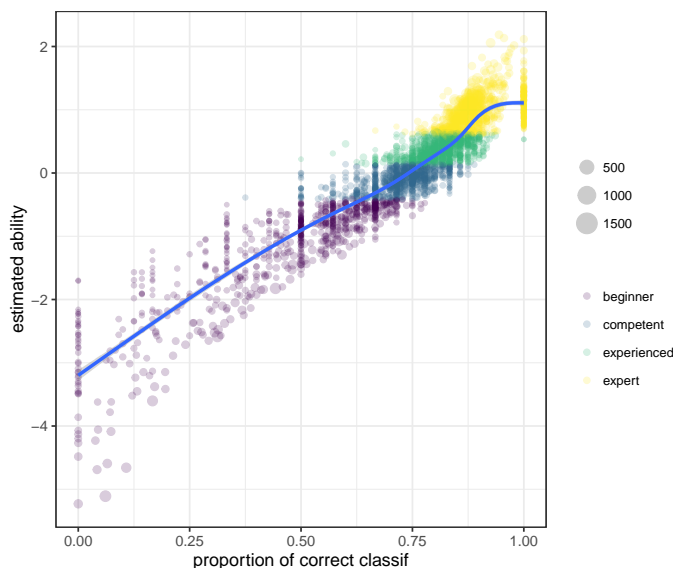


Figure 8: Posterior estimates of the users’ abilities vs their proportion of correct classifications. The size of the dots represents the users’ number of classifications.

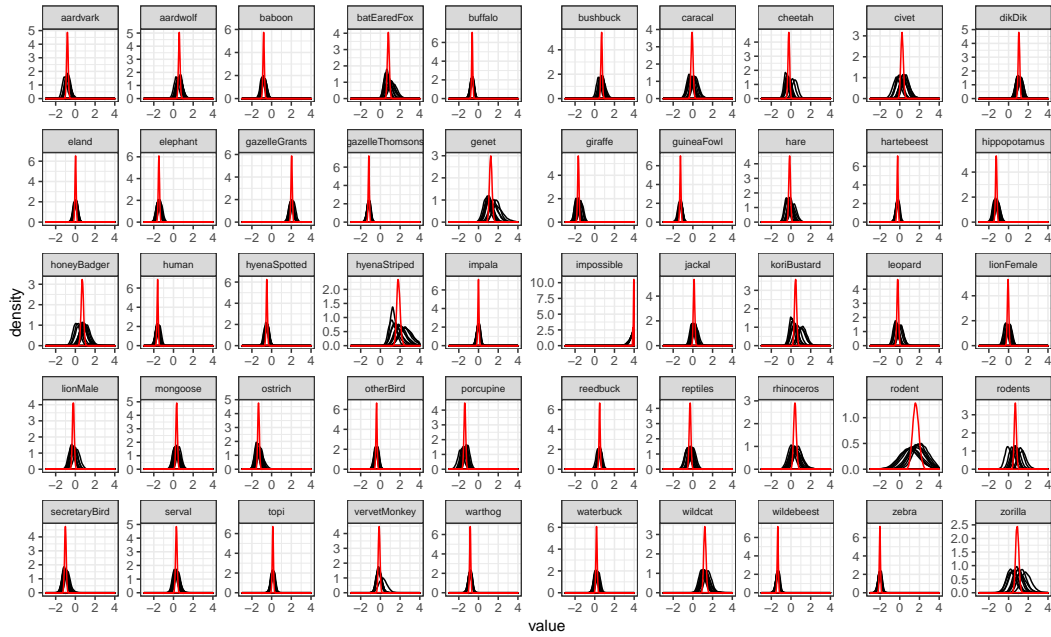
data produced by citizens and hence by these programs are generally inaccurate and/or imprecise, which has received a lot of attention in recent years. Prior research has also noted the importance of measuring the contribution of the subjects to citizen science projects (Silvertown et al., 2015). Although item-response models provide a natural framework in which to investigate and perhaps adjust for these challenges, the literature is limited on their usefulness for crowdsourced programs.

In this research, we introduced a new methodology and family of IRT models specially tailored for ecological applications. We focus on spatial data frequently collected in citizen science applications and specifically on citizen-elicited annotations of images. We discuss the application of these models for real-world data, specifically in the presence of inconveniently large datasets. We found that our proposed framework of modeling outperforms the benchmark method in terms of precision and accuracy in a simulation experiment considering factors like the number of geotagged locations, the number of participants, etc. Similarly, our approach performed better for real-life data. The application of the divide-and-recombine approach for massive item response problems is novel and can be translated and extended to other settings.

Our methodology provides a better way of assessing the proficiency of the participants, which is useful for comparing them on equal grounds, for measuring their contribution, for building reputation schemes and for compensation purposes. It also identifies challenging and commonly misclassified classes of responses (e.g. species) in order to produce better guidance for the users and training. Obtaining difficulties associated with images gives indications of cameras technical malfunctioning, misplacement, light conditions, etc.

In our models, participants’ abilities were considered to be constant across the classification period. This is reasonable since the period is generally short for many citizen science projects. However, in some circumstances this condition does not hold, e.g. an increased level of skill is achieved with time as participants learn and train. Consequently, variations like those suggested in Martin and Quinn (2002); Dunson (2003); Wang et al. (2013) and Weng et al. (2018) can be adopted. Furthermore, other methods accounting for the participants’ reaction times could also be explored Zhan et al. (e.g. 2018); Fox (e.g. 2010). Potential extensions of this particular case

(a) Subposterior estimates of the species difficulties



(b) Species difficulties vs the proportion of correct classification

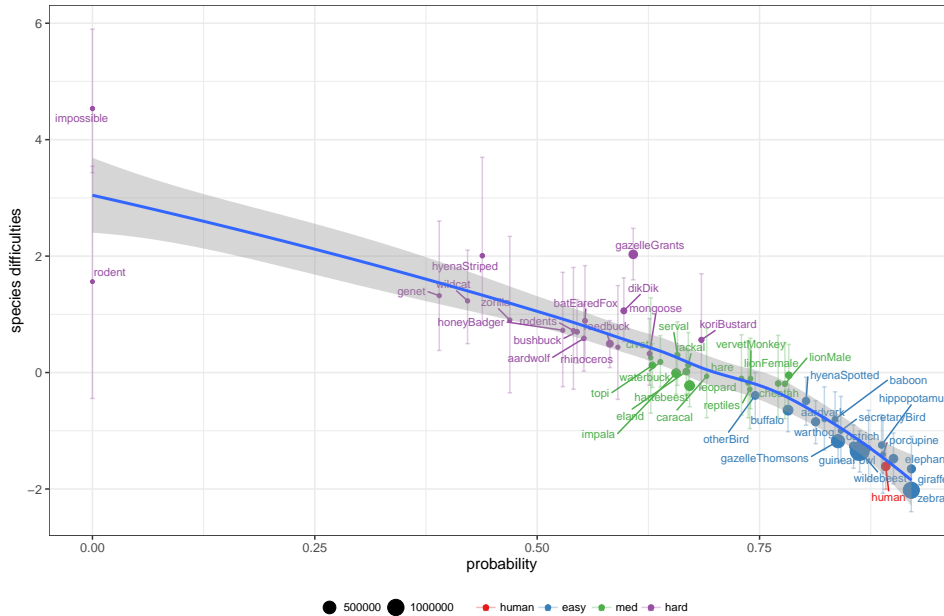
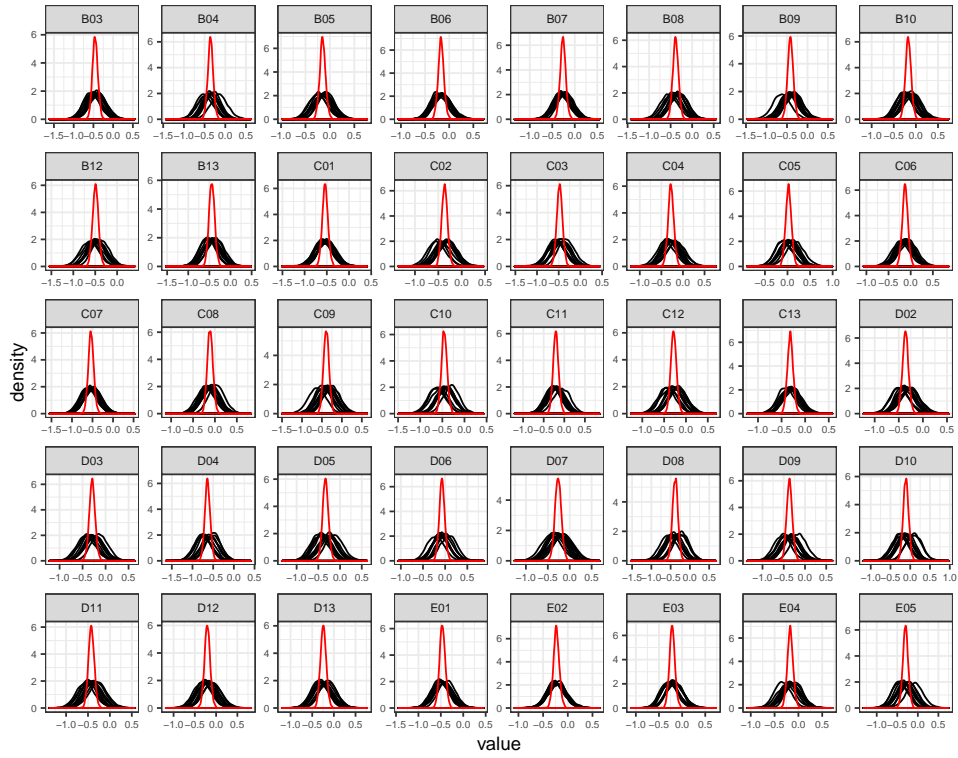


Figure 9: (a) Comparisons of the subposterior estimates of the species difficulties from the 10 subsets and from the consensus Monte Carlo (in red color) in the 50 species. (b) Species difficulties and 95% highest posterior density interval as a function of the proportion of species correct classification. The size of the dots represents the number of times a given species is presented for classification. The category *human* is used as a baseline.

(a) Subposterior estimates of the site difficulties



(b) Site difficulties vs the proportion of correct classification

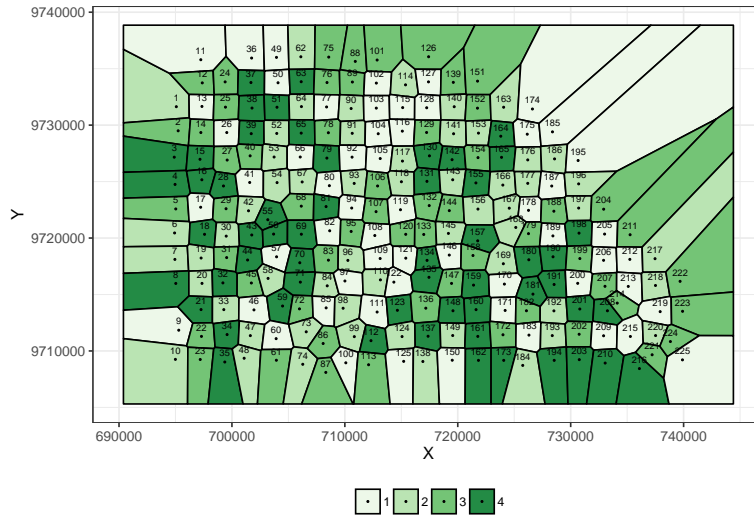


Figure 11: (a) Comparisons of the difficulties posterior estimates in the first 40 sites in the subsets and compared to the consensus estimate. (b) Voronoi diagram of the posterior estimates of the site-related difficulties. Four categories were obtained using the quantiles where dark (light) green represent more difficult (easier) sites. Dots represent the location of the camera.

study based on the classification of camera traps images include accounting for covariates affecting the species difficulties such as the presence of young specimens or captured while moving. Camera-specific parameters and time of the day that also impact the quality of the photograph could be included as a factor in the model. In terms of scalability, variational approximations could be used to speed up the computation on big datasets (Natesan et al., 2016; Hui et al., 2017). We are currently exploring an online updating approach for processing data as it becomes available (Schifano et al., 2016; Särkkä, 2013).

SUPPLEMENTARY MATERIAL

The supplementary material includes the following files:

Simulations results and posterior estimates obtained via consensus Monte Carlo.

Serengeti data set: Dataset used in Section 4.3. (serengeti.RDS file) <https://github.com/the-anonymous-author/Item-Response-JASA>

Codes used in Item response modeling for big data: R markdown file containing the R codes and Stan codes used in Section 4.3.

References

- Albert, J. (2015). Introduction to Bayesian item response modelling. *International Journal of Quantitative Research in Education* 2(3-4), 178–193.
- Albert, J. H. (1992). Bayesian estimation of normal ogive item response curves using Gibbs sampling. *Journal of educational statistics* 17(3), 251–269.
- Bachrach, Y., T. Graepel, T. Minka, and J. Guiver (2012). How to grade a test without knowing the answers—a Bayesian graphical model for adaptive crowdsourcing and aptitude testing. *arXiv preprint arXiv:1206.6386*.
- Baker, F. B. and S.-H. Kim (2004). *Item response theory: Parameter estimation techniques*. CRC Press.
- Besag, J., J. York, and A. Molli (1991). Bayesian image restoration, with two applications in spatial statistics. *Annals of the Institute of Statistical Mathematics* 43(1), 120.
- Bird, T. J., A. E. Bates, J. S. Lefcheck, N. A. Hill, R. J. Thomson, G. J. Edgar, R. D. Stuart-Smith, S. Wotherspoon, M. Krkosek, J. F. Stuart-Smith, G. T. Pecl, N. Barrett, and S. Frusher (2014). Statistical solutions for error and bias in global citizen science datasets. *Biological Conservation* 173, 144 – 154.
- Birnbaum, L. (1968). Some latent trait models and their use in inferring an examinee’s ability. In *Statistical theories of mental test scores*. Addison-Wesley.
- Bonney, R., C. B. Cooper, J. Dickinson, S. Kelling, T. Phillips, K. V. Rosenberg, and J. Shirk (2009). Citizen science: a developing tool for expanding science knowledge and scientific literacy. *BioScience* 59(11), 977–984.

- Bonney, R., J. L. Shirk, T. B. Phillips, A. Wiggins, H. L. Ballard, A. J. Miller-Rushing, and J. K. Parrish (2014). Next steps for citizen science. *Science* 343(6178), 1436–1437.
- Bürkner, P.-C. (2019). Bayesian Item Response Modelling in R with brms and Stan. *arXiv preprint arXiv:1905.09501*.
- Cai, L., K. Choi, M. Hansen, and L. Harrell (2016). Item response theory. *Annual Review of Statistics and Its Application* 3(1), 297–321.
- Callaghan, C. T., J. J. Rowley, W. K. Cornwell, A. G. Poore, and R. E. Major (2019). Improving big citizen science data: Moving beyond haphazard sampling. *PLOS Biology* 17(6), e3000357.
- Cançado, A. L., A. E. Gomes, C. Q. da Silva, F. L. Oliveira, and L. H. Duczmal (2016). An item response theory approach to spatial cluster estimation and visualization. *Environmental and ecological statistics* 23(3), 435–451.
- Carpenter, B., A. Gelman, M. D. Hoffman, D. Lee, B. Goodrich, M. Betancourt, M. Brubaker, J. Guo, P. Li, and A. Riddell (2017). Stan: A probabilistic programming language. *Journal of statistical software* 76(1).
- Chalmers, R. P. (2012). mirt: A multidimensional item response theory package for the R environment. *Journal of Statistical Software* 48(6), 1–29.
- Chambert, T., E. H. C. Grant, D. A. Miller, J. D. Nichols, K. P. Mulder, and A. B. Brand (2018). Two-species occupancy modelling accounting for species misidentification and non-detection. *Methods in Ecology and Evolution* 9(6), 1468–1477.
- Choy, S. L., R. O’Leary, and K. Mengersen (2009). Elicitation by design in ecology: using expert opinion to inform priors for bayesian statistical models. *Ecology* 90(1), 265–277.
- Curtis, S. M. et al. (2010). BUGS code for item response theory. *Journal of Statistical Software* 36(1), 1–34.
- Datta, A., S. Banerjee, A. O. Finley, and A. E. Gelfand (2016). Hierarchical nearest-neighbor Gaussian process models for large geostatistical datasets. *Journal of the American Statistical Association* 111(514), 800–812.
- De Ayala, R. J. (2013). *The theory and practice of item response theory*. Guilford Publications.
- De Jong, M. G., R. Pieters, and J.-P. Fox (2010). Reducing social desirability bias through item randomized response: An application to measure underreported desires. *Journal of Marketing Research* 47(1), 14–27.
- Dennis, E. B., B. J. Morgan, S. N. Freeman, M. S. Ridout, T. M. Brereton, R. Fox, G. D. Powney, and D. B. Roy (2017). Efficient occupancy model-fitting for extensive citizen-science data. *PloS one* 12(3), e0174433.
- Dunson, D. B. (2003). Dynamic latent trait models for multidimensional longitudinal data. *Journal of the American Statistical Association* 98(463), 555–563.
- Embretson, S. E. and S. P. Reise (2013). *Item response theory*. Psychology Press.

- Falk, S., G. Foster, R. Comont, J. Conroy, H. Bostock, A. Salisbury, D. Kilbey, J. Bennett, and B. Smith (2019). Evaluating the ability of citizen scientists to identify bumblebee (*bombus*) species. *PloS one* 14(6), e0218614.
- Finley, A. O., A. Datta, B. C. Cook, D. C. Morton, H. E. Andersen, and S. Banerjee (2017). Applying nearest neighbor Gaussian processes to massive spatial data sets forest canopy height prediction across Tanana Valley Alaska. *arXiv preprint arXiv:1702.00434*.
- Fischer, G. H. (1973). The linear logistic test model as an instrument in educational research. *Acta psychologica* 37(6), 359–374.
- Fox, J.-P. (2010). *Bayesian item response modeling: Theory and applications*. Springer Science & Business Media.
- Fritz, S., L. See, T. Carlson, M. M. Haklay, J. L. Oliver, D. Fraisl, R. Mondardini, M. Brocklehurst, L. A. Shanley, S. Schade, et al. (2019). Citizen science and the United Nations Sustainable Development Goals. *Nature Sustainability* 2(10), 922–930.
- Gadermann, A. M., M. Guhn, and B. D. Zumbo (2012). Estimating ordinal reliability for likert-type and ordinal item response data: a conceptual, empirical, and practical guide. *Practical Assessment, Research & Evaluation* 17(3).
- Grant, R. L., D. C. Furr, B. Carpenter, and A. Gelman (2016). Fitting Bayesian item response models in Stata and Stan. *arXiv preprint arXiv:1601.03443*.
- Gura, T. (2013). Citizen science: amateur experts. *Nature* 496(7444), 259–261.
- Hoffman, M. D. and A. Gelman (2014). The No-U-turn sampler: adaptively setting path lengths in Hamiltonian Monte Carlo. *Journal of Machine Learning Research* 15(1), 1593–1623.
- Howe, J. (2008). *Crowdsourcing: How the power of the crowd is driving the future of business*. Random House.
- Hsing, P.-Y., S. Bradley, V. T. Kent, R. A. Hill, G. C. Smith, M. J. Whittingham, J. Cokill, D. Crawley, M. volunteers, and P. A. Stephens (2018). Economical crowdsourcing for camera trap image classification. *Remote Sensing in Ecology and Conservation* 4(4), 361–374.
- Hsu, A., O. Malik, L. Johnson, and D. C. Esty (2014). Development: Mobilize citizens to track sustainability. *Nature News* 508(7494), 33.
- Hui, F. K., D. I. Warton, J. T. Ormerod, V. Haapaniemi, and S. Taskinen (2017). Variational approximations for generalized linear latent variable models. *Journal of Computational and Graphical Statistics* 26(1), 35–43.
- Juhl, S. (2019). Measurement uncertainty in spatial models: A Bayesian dynamic measurement model. *Political Analysis* 27(3), 302–319.
- Katzfuss, M. and N. Cressie (2012). Bayesian hierarchical spatio-temporal smoothing for very large datasets. *Environmetrics* 23(1), 94–107.
- Kelling, S., A. Johnston, W. M. Hochachka, M. Iliff, D. Fink, J. Gerbracht, C. Lagoze, F. A. La Sorte, T. Moore, A. Wiggins, et al. (2015). Can observation skills of citizen scientists be estimated using species accumulation curves? *PLoS One* 10(10), e0139600.

- Kohler, K. E. and S. M. Gill (2006). Coral point count with excel extensions (cpce): A visual basic program for the determination of coral and substrate coverage using random point count methodology. *Computers & Geosciences* 32(9), 1259–1269.
- Kosmala, M., K. Hufkens, and A. D. Richardson (2018). Integrating camera imagery, crowdsourcing, and deep learning to improve high-frequency automated monitoring of snow at continental-to-global scales. *PloS one* 13(12), e0209649.
- Kosmala, M., A. Wiggins, A. Swanson, and B. Simmons (2016). Assessing data quality in citizen science. *Frontiers in Ecology and the Environment* 14(10), 551–560.
- Laurens, K. R., M. Hobbs, M. Sunderland, M. J. Green, and G. Mould (2012). Psychotic-like experiences in a community sample of 8000 children aged 9 to 11 years: an item response theory analysis. *Psychological medicine* 42(7), 1495–1506.
- Lord, F. M. (1980). *Applications of item response theory to practical testing problems*. Hillsdale, NJ:Erlbaum.
- Luo, Y. and H. Jiao (2018). Using the Stan program for Bayesian item response theory. *Educational and psychological measurement* 78(3), 384–408.
- Martin, A. D. and K. M. Quinn (2002). Dynamic ideal point estimation via Markov chain Monte Carlo for the US Supreme Court, 1953–1999. *Political Analysis* 10(2), 134–153.
- McGann, A. J. (2014). Estimating the political center from aggregate data: an item response theory alternative to the stinson dyad ratios algorithm. *Political Analysis* 22(1), 115–129.
- McKinley, D. C., A. J. Miller-Rushing, H. L. Ballard, R. Bonney, H. Brown, S. C. Cook-Patton, D. M. Evans, R. A. French, J. K. Parrish, T. B. Phillips, et al. (2017). Citizen science can improve conservation science, natural resource management, and environmental protection. *Biological Conservation* 208, 15–28.
- Mengersen, K., E. E. Peterson, S. Clifford, N. Ye, J. Kim, T. Bednarz, R. Brown, A. James, J. Vercelloni, A. R. Pearse, et al. (2017). Modelling imperfect presence data obtained by citizen science. *Environmetrics* 28(5), e2446.
- Meyer, J. P. and S. Zhu (2013). Fair and equitable measurement of student learning in MOOCs: An introduction to item response theory, scale linking, and score equating. *Research & Practice in Assessment* 8, 26–39.
- Miroshnikov, A. and E. Conlon (2014). *parallelMCMCcombine: Methods for combining independent subset Markov chain Monte Carlo (MCMC) posterior samples to estimate a posterior density given the full data set*. R package version 1.0.
- Mislevy, R. J. (1986). Bayes modal estimation in item response models. *Psychometrika* 51(2), 177–195.
- Morris, M., K. Wheeler-Martin, D. Simpson, S. J. Mooney, A. Gelman, and C. DiMaggio (2019). Bayesian hierarchical spatial models: Implementing the besag york mollié model in stan. *Spatial and spatio-temporal epidemiology* 31, 100301.

- Natesan, P., R. Nandakumar, T. Minka, and J. D. Rubright (2016). Bayesian prior choice in IRT estimation using MCMC and variational Bayes. *Frontiers in psychology* 7, 1422.
- Neiswanger, W., C. Wang, and E. Xing (2013). Asymptotically exact, embarrassingly parallel MCMC. *arXiv preprint arXiv:1311.4780*.
- Patz, R. J. and B. W. Junker (1999). Applications and extensions of mcmc in irt: Multiple item types, missing data, and rated responses. *Journal of educational and behavioral statistics* 24(4), 342–366.
- Peterson, E. E., E. Santos-Fernandez, C. Chen, S. Clifford, J. Vercelloni, A. Pearse, R. Brown, B. Christensen, A. James, K. Anthony, J. Loder, M. Gonzalez-Rivero, C. Roelfsema, M. J. Caley, C. Mellin, T. Bednarz, and K. Mengersen (2019). Monitoring through many eyes: Integrating disparate datasets to improve monitoring of the Great Barrier Reef. *Environmental Modelling & Software*, 104557.
- Pollock, L. J., R. Tingley, W. K. Morris, N. Golding, R. B. O’Hara, K. M. Parris, P. A. Vesik, and M. A. McCarthy (2014). Understanding co-occurrence by modelling species simultaneously with a Joint Species Distribution Model (JSDM). *Methods in Ecology and Evolution* 5(5), 397–406.
- Rasch, G. (1960). *Studies in mathematical psychology: I. Probabilistic models for some intelligence and attainment tests*. Nielsen & Lydiche. Oxford, England.
- Ratnieks, F. L., F. Schrell, R. C. Sheppard, E. Brown, O. E. Bristow, and M. Garbuzov (2016). Data reliability in citizen science: learning curve and the effects of training method, volunteer background and experience on identification accuracy of insects visiting ivy flowers. *Methods in Ecology and Evolution* 7(10), 1226–1235.
- Raykar, V. C., S. Yu, L. H. Zhao, G. H. Valadez, C. Florin, L. Bogoni, and L. Moy (2010). Learning from crowds. *Journal of Machine Learning Research* 11(Apr), 1297–1322.
- Samejima, F. (1969). Estimation of latent ability using a response pattern of graded scores. *Psychometrika monograph supplement*.
- Särkkä, S. (2013). *Bayesian filtering and smoothing*, Volume 3. Cambridge University Press.
- Schifano, E. D., J. Wu, C. Wang, J. Yan, and M.-H. Chen (2016). Online updating of statistical inference in the big data setting. *Technometrics* 58(3), 393–403.
- Scott, S. L., A. W. Blocker, F. V. Bonassi, H. A. Chipman, E. I. George, and R. E. McCulloch (2016). Bayes and big data: The consensus Monte Carlo algorithm. *International Journal of Management Science and Engineering Management* 11(2), 78–88.
- Silvertown, J., M. Harvey, R. Greenwood, M. Dodd, J. Rosewell, T. Rebelo, J. Ansine, and K. McConway (2015). Crowdsourcing the identification of organisms: A case-study of iSpot. *ZooKeys* (480), 125.
- Stone, C. A. and X. Zhu (2015). *Bayesian analysis of item response theory models using SAS*. Sas Institute.

- Sullivan, B. L., C. L. Wood, M. J. Iliff, R. E. Bonney, D. Fink, and S. Kelling (2009). ebird: A citizen-based bird observation network in the biological sciences. *Biological Conservation* 142(10), 2282–2292.
- Swanson, A., M. Kosmala, C. Lintott, R. Simpson, A. Smith, and C. Packer (2015). Snapshot Serengeti, high-frequency annotated camera trap images of 40 mammalian species in an African savanna. *Scientific data* 2, 150026.
- van der Linden, W. J. and R. K. Hambleton (2013). *Handbook of modern item response theory*. Springer Science & Business Media.
- van der Linden, W. J., R. H. Klein Entink, and J.-P. Fox (2010). IRT parameter estimation with response times as collateral information. *Applied Psychological Measurement* 34(5), 327–347.
- Vehtari, A., A. Gelman, and J. Gabry (2017). Practical Bayesian model evaluation using leave-one-out cross-validation and WAIC. *Statistics and computing* 27(5), 1413–1432.
- Wang, C., M.-H. Chen, E. Schifano, J. Wu, and J. Yan (2016). Statistical methods and computing for big data. *Statistics and its interface* 9(4), 399.
- Wang, X., J. O. Berger, D. S. Burdick, et al. (2013). Bayesian analysis of dynamic item response models in educational testing. *The Annals of Applied Statistics* 7(1), 126–153.
- Warton, D. I., F. G. Blanchet, R. B. OHara, O. Ovaskainen, S. Taskinen, S. C. Walker, and F. K. Hui (2015). So many variables: joint modeling in community ecology. *Trends in Ecology & Evolution* 30(12), 766–779.
- Watanabe, S. (2010). Asymptotic equivalence of bayes cross validation and widely applicable information criterion in singular learning theory. *Journal of Machine Learning Research* 11(Dec), 3571–3594.
- Wauters, K., P. Desmet, and W. Van Den Noortgate (2010). Adaptive item-based learning environments based on the item response theory: possibilities and challenges. *Journal of Computer Assisted Learning* 26(6), 549–562.
- Weng, R. C.-H., D. S. Coad, et al. (2018). Real-time Bayesian parameter estimation for item response models. *Bayesian Analysis* 13(1), 115–137.
- Willi, M., R. T. Pitman, A. W. Cardoso, C. Locke, A. Swanson, A. Boyer, M. Veldthuis, and L. Fortson (2019). Identifying animal species in camera trap images using deep learning and citizen science. *Methods in Ecology and Evolution* 10(1), 80–91.
- Wilson, M., P. De Boeck, and C. H. Carstensen (2008). Explanatory item response models: A brief introduction. *Assessment of competencies in educational contexts*, 91–120.
- Zhan, P., H. Jiao, and D. Liao (2018). Cognitive diagnosis modelling incorporating item response times. *British Journal of Mathematical and Statistical Psychology* 71(2), 262–286.
- Zhang, J., K. Huang, M. Cottman-Fields, A. Truskinger, P. Roe, S. Duan, X. Dong, M. Towsey, and J. Wimmer (2013). Managing and analysing big audio data for environmental monitoring. In *2013 IEEE 16th International Conference on Computational Science and Engineering*, pp. 997–1004. IEEE.

S.6 SUPPLEMENTARY MATERIAL: Simulations results and posterior estimates obtained via consensus Monte Carlo

Summary: This is the supplementary material for Bayesian item response models for citizen science ecological data and it is composed of two sections. Section S.6.1 contains information supporting the simulation study. Some results regarding the Case Study are presented in Section S.6.2.

S.6.1 Simulations results.

In section 3.2 we performed a simulation study to compare both models. Fig.S.12a and S.12b depict the posterior distributions violin and boxplots for the abilities in both models (3PL vs 3PLUS) as a function of the true fixed value given by the red dots.

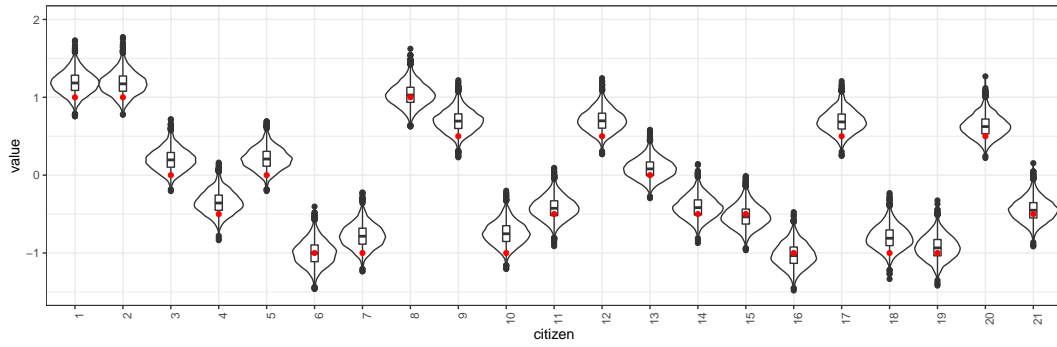
S.6.2 Posterior estimates from the subposteriors via consensus Monte Carlo.

In the case study (section 4.3), we split the big dataset and fit the Bayesian item response model to each of the individual shards. Fig S.13 shows a comparison of the ability estimates in the 10 shards and those obtained from the consensus Monte Carlo approach.

Similar comparisons are shown in Fig S.14, S.15 and S.16 for the difficulties associated to the species, the pseudoguessing and the site difficulties respectively.

Table S.3 shows the consensus posterior estimates for some of the parameters of interest.

(a) 3PL



(b) 3PLUS

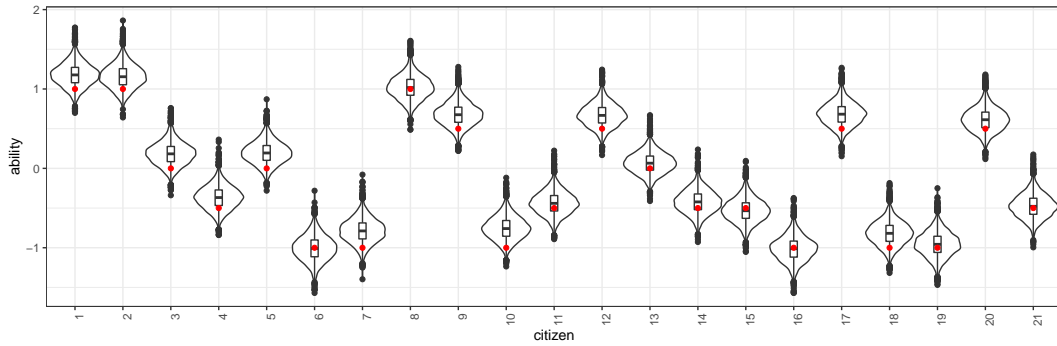


Figure S.12: Violin/box plot of the posterior distribution of the five groups of users' abilities θ_j in the 3PL (a) and 3PLUS model (b). The red dots represent the fixed true abilities.

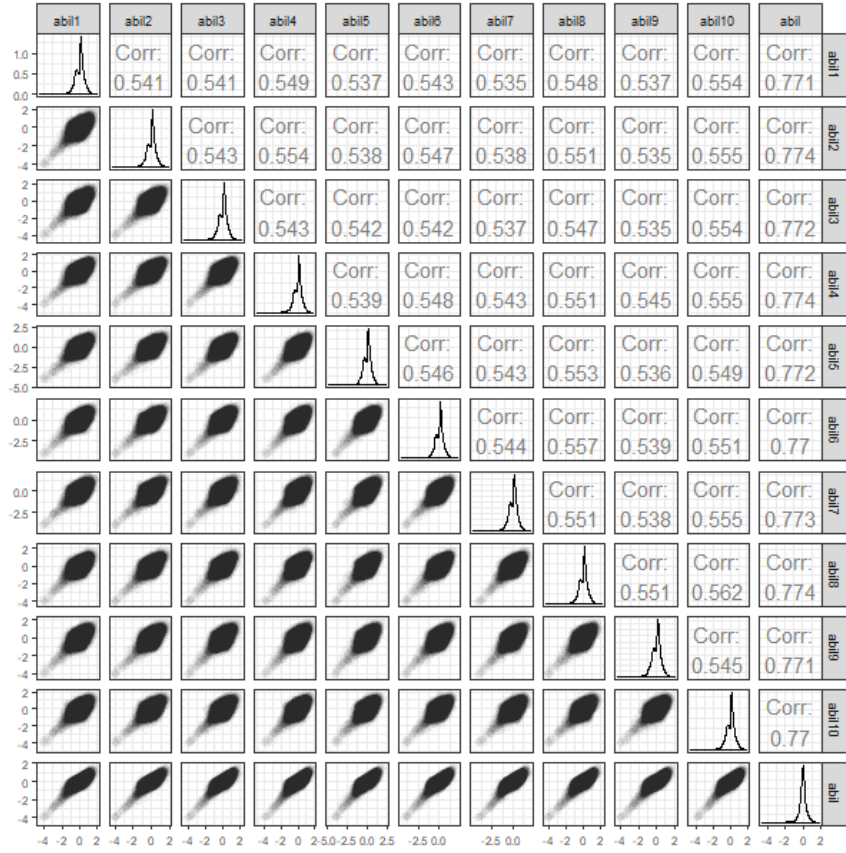


Figure S.13: Comparison of the posterior estimates in the 21,347 users abilities in the shards and from the consensus approach.

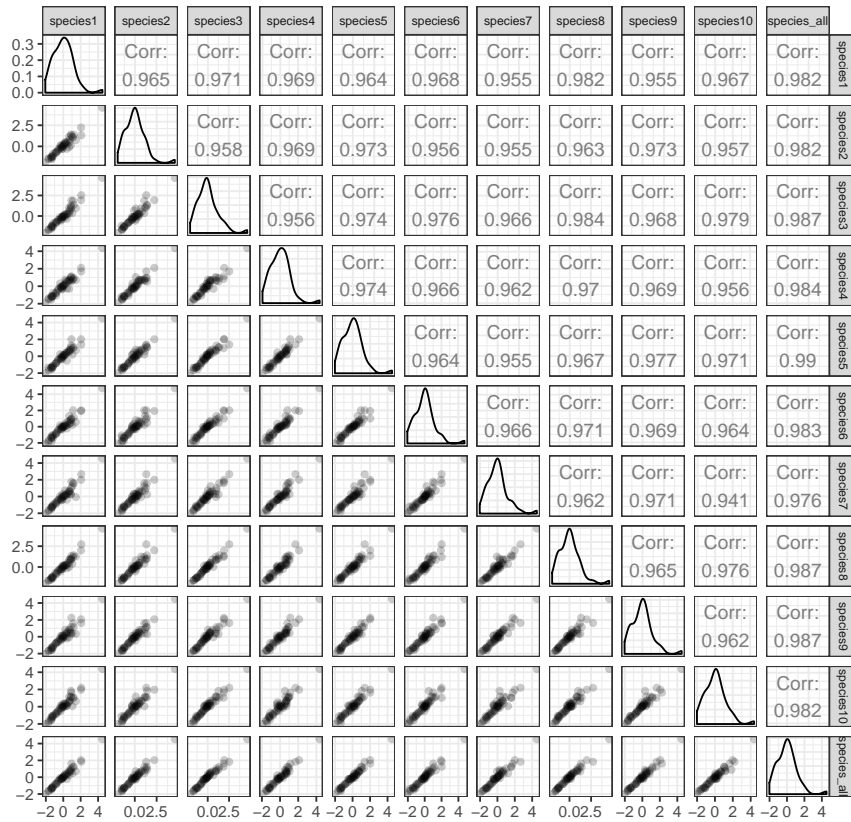


Figure S.14: Comparisons of the posterior estimates of the species difficulties in the shards and from the consensus approach (species_all).

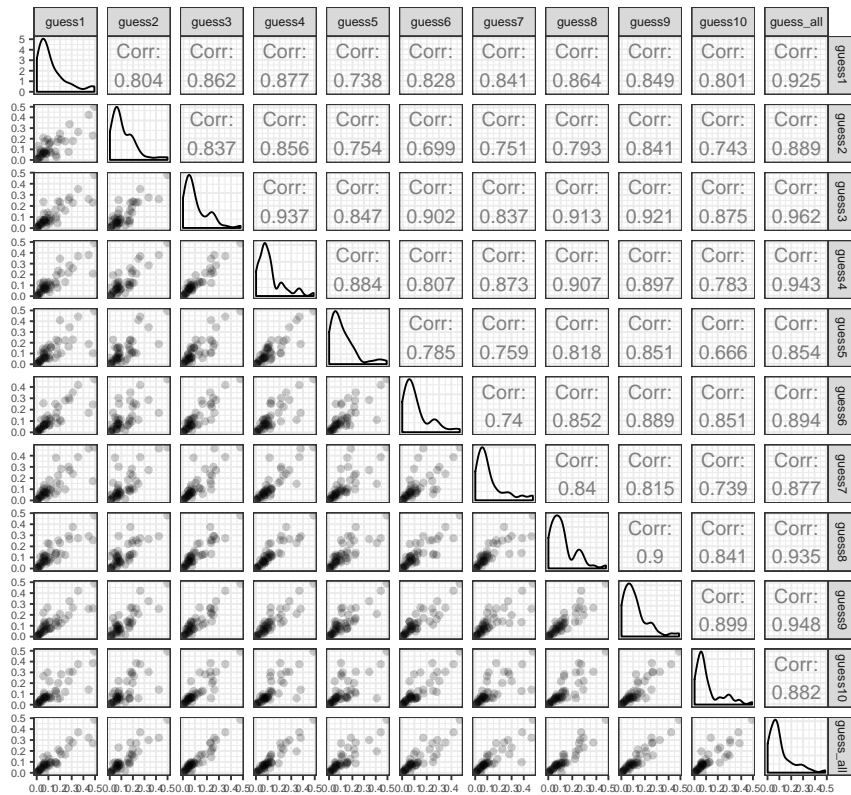


Figure S.15: Comparisons of the posterior means estimates of the species pseudoguessing in the subsets and compared to the combined estimate (guess_all).

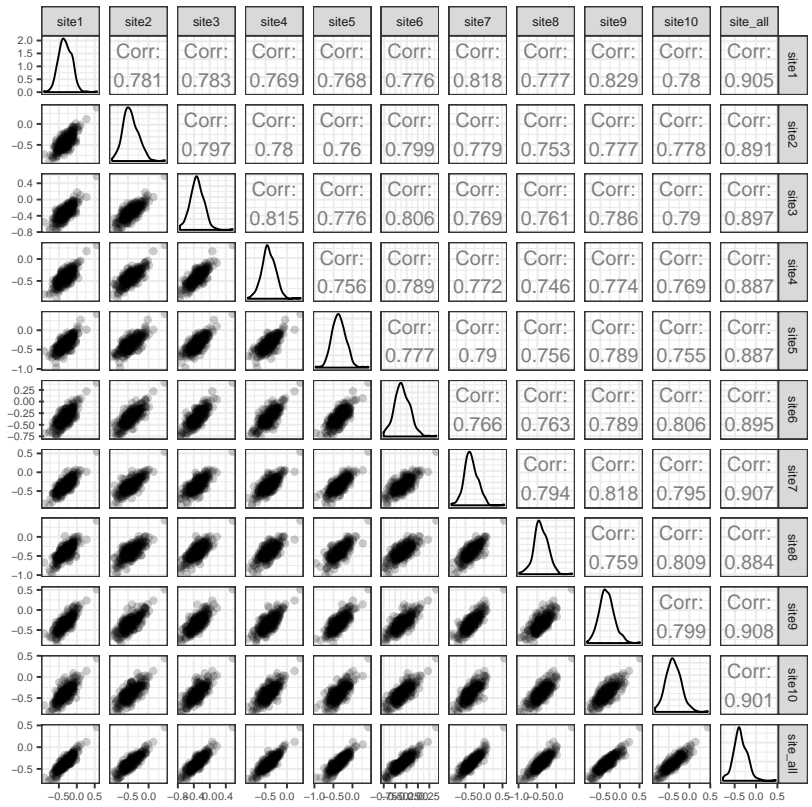


Figure S.16: Comparisons of the difficulties posterior estimates in the 10 subsets (site1, site2, etc) and compared to the consensus estimate (site_all).

Table S.3: Posterior estimates of some of the parameters via consensus Monte Carlo.

	param	id	mean	sd	med	$q_{2.5}$	$q_{97.5}$
1	diff_species_3	baboon	-0.802	0.229	-0.807	-1.251	-0.331
2	diff_species_24	hyenaStriped	2.007	0.734	1.902	0.842	3.697
3	diff_species_26	impossible	4.535	0.614	4.495	3.433	5.898
4	diff_species_30	lionFemale	-0.046	0.267	-0.046	-0.585	0.482
5	diff_species_49	zebra	-2.020	0.180	-2.019	-2.390	-1.671
6	diff_site_1	B03	-0.456	0.214	-0.456	-0.882	-0.023
7	diff_site_2	B04	-0.359	0.216	-0.360	-0.788	0.085
8	diff_site_3	B05	-0.151	0.190	-0.150	-0.527	0.237
9	diff_site_4	B06	-0.167	0.183	-0.169	-0.526	0.208
10	pseudoguessing_3	baboon	0.137	0.083	0.127	0.009	0.322
11	pseudoguessing_24	hyenaStriped	0.230	0.100	0.241	0.019	0.397
12	pseudoguessing_26	impossible	0.010	0.009	0.007	0.000	0.034
13	pseudoguessing_30	lionFemale	0.366	0.074	0.373	0.203	0.497
14	pseudoguessing_49	zebra	0.009	0.009	0.007	0.000	0.032
15	abil_1	1ee963bb67658ec7fb7ff5568f2e5c52	1.016	0.587	0.981	-0.052	2.288
16	abil_2	43047c40867c00a83d0a3982f12f515b	-0.446	0.822	-0.443	-2.128	1.191
17	abil_3	52a791d0b1715d3a64e3304853d78c7c	1.019	0.386	0.978	0.353	1.893
18	abil_4	6ed2e808d62f729c45912856bffb1ae7	0.000	0.592	-0.040	-1.067	1.315
19	abil_5	80c3e443a01284ce8be767b3b68b921d	1.176	0.354	1.143	0.555	1.958
20	abil_6	b1132cb9f684ac9bf8b08522c7537ea6	-0.041	0.528	-0.069	-1.020	1.122
21	abil_7	cb7671ced14ad6f669a2601b249e0e93	-1.407	0.580	-1.402	-2.594	-0.252
22	abil_8	cb93d3701ea002dd736828eb1a87cb88	-0.880	0.616	-0.884	-2.107	0.363
23	abil_9	e6b9208fb9d03ce1c3885fbb866a39f8	0.226	0.458	0.200	-0.620	1.200